



ELSEVIER

Journal of Physics and Chemistry of Solids 63 (2002) 1343–1346

JOURNAL OF
PHYSICS AND CHEMISTRY
OF SOLIDS

www.elsevier.com/locate/jpcs

Dynamics of orbital degree of freedom in transition-metal oxides

S. Ishihara^{a,*}, S. Okamoto^b, S. Maekawa^c^aDepartment of Applied Physics, University of Tokyo, Tokyo 113-8656, Japan^bThe Institute of Physical and Chemical Research (RIKEN), Saitama 351-0198, Japan^cInstitute for Materials Research, Tohoku University, Sendai 980-8577, Japan

Abstract

The collective excitation in the orbital degree of freedom termed orbital wave is studied in the orbital ordered transition-metal oxides, in particular, in LaMnO₃. Symmetry, dispersion and energy gap of this excitation are examined by the group theoretical analyses and the linear spin-wave theory. The cross-section of the Raman scattering from the orbital wave is calculated and is compared with the recent experimental results. © 2002 Elsevier Science Ltd. All rights reserved.

Keywords: A. Magnetic material; C. Raman spectroscopy; D. Optical properties; D. Magnetic properties

1. Introduction

Orbital degree of freedom and its interplay with spin, charge and lattice degrees of freedom are one of the central issues in transition-metal oxides. The electronic orbital in transition-metal oxides has been studied for more than 40 years. In particular, the orbital degree of freedom has been investigated in connection with the superexchange interaction between spins and the cooperative Jahn–Teller effects. After the discovery of the colossal magnetoresistive manganites with perovskite crystal structure, study of the orbital degree of freedom has been revived. One of the new points in this research field is dynamics of the orbital degree of freedom [1]. The orbital is a quantum variable of an electron, as spin and charge degrees of freedom are, and this has its own dynamics. This is termed orbital excitations/fluctuations.

Let us focus on the orbital excitations in orbital ordered LaMnO₃ where one of the doubly degenerate e_g orbitals, i.e. 3d_{3z²-r²} and 3d_{x²-y²} orbitals are occupied by an electron in each Mn ion. The orbital degree of freedom at site *i* is mathematically described by the pseudo-spin operator \vec{T}_i with quantum number $T = 1/2$. The up and down pseudo-

spin states correspond to the states where 3d_{3z²-r²} and 3d_{x²-y²} orbitals are occupied by an electron, respectively. Below 780 K, 3d_{3x²-r²} and 3d_{3y²-r²} orbitals are alternately ordered in the *xy* plane [2]. The orbital order parameter is identified as $\langle \vec{T}_k \rangle = ((\sqrt{3}/4)\delta_{k=(\pi,\pi,0)}, 0, -1/4\delta_{k=(0,0,0)})$, where \vec{T}_k is the Fourier transform of \vec{T}_i and $\langle \dots \rangle$ indicates the thermal average. The orbital excitation in the orbital ordered state is represented by deviations of \vec{T}_i from the above value. In particular, the collective orbital excitation in the orbital ordered state is termed the orbital wave (OW). This is analogous to the spin wave in the magnetically ordered states and propagates by interaction between orbitals at different sites.

We report, in this paper, the theoretical results of the orbital excitations in orbital ordered transition-metal oxides. In particular, we focus on the collective orbital excitations in LaMnO₃ and its dispersion relation and symmetry. The Raman spectra from the orbital excitations are calculated and the results are compared with the recent experiments.

2. Orbital wave in perovskite manganites

The dispersion relation of OW is governed by the interaction between orbitals at different sites. Among several kinds of interactions between orbitals, one of the dominant interactions is caused by the virtual electron hopping between Mn sites under the strong on-site Coulomb interaction. This interaction is described by the following

* Corresponding author. Tel.: +81-3-5841-6816; fax: +81-3-5841-8802.

E-mail address: ishihara@ap.t.u-tokyo (S. Ishihara).

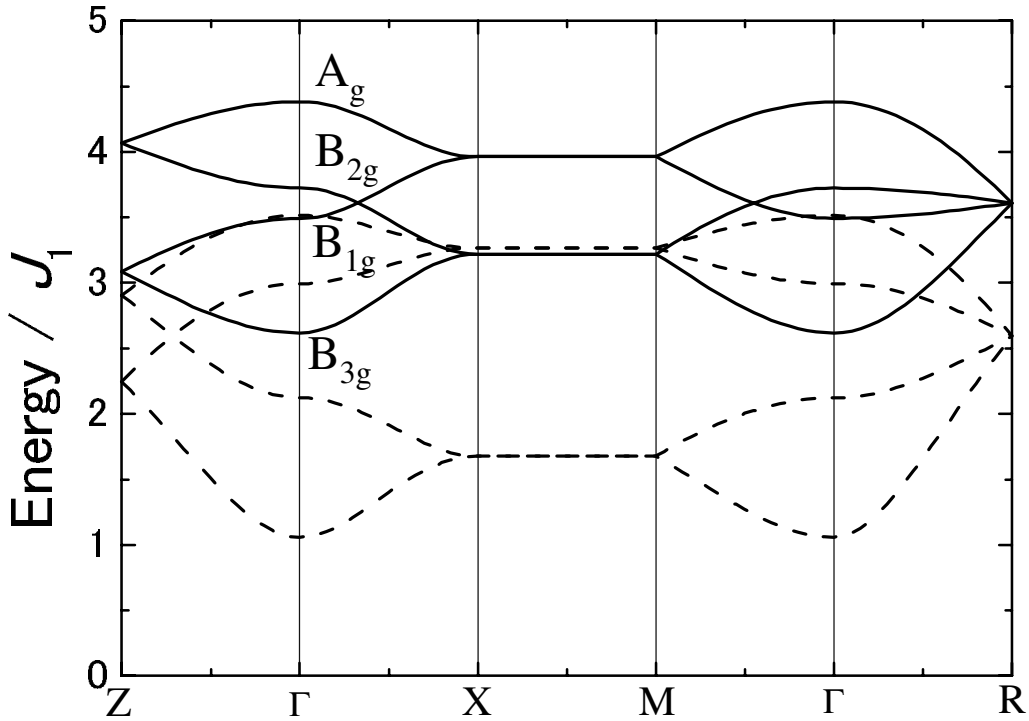


Fig. 1. Dispersion relation of the OW in the A-type AF phase (solid curves) and the paramagnetic phase (dotted curves).

Hamiltonian [3,4];

$$\mathcal{H} = -2J_1 \sum_{\langle ij \rangle} \left(\frac{1}{4} - \vec{S}_i \cdot \vec{S}_j \right) \left(\frac{1}{4} - \tau_i^l \tau_j^l \right) - 2J_2 \sum_{\langle ij \rangle} \left(\frac{3}{4} + \vec{S}_i \cdot \vec{S}_j \right) \left(\frac{3}{4} + \tau_i^l \tau_j^l + \tau_i^l + \tau_j^l \right), \quad (1)$$

where $\tau_i^l = \cos(2\pi m_l/3)T_{iz} - \sin(2\pi m_l/3)T_{ix}$ with $(m_x, m_y, m_z) = (1, 2, 3)$ and l denotes the direction of a bond connecting a site i and its nearest neighboring (NN) site j . \vec{S} is the spin operator with quantum number $S = 1/2$. Two terms in \mathcal{H} correspond to the different exchange processes and (J_1, J_2) are amplitudes of these interactions. The exchange of virtual phonons also causes the interaction between orbitals and is interpreted to be included in Eq. (1). This is because this process provides the same form of the orbital interaction with that in Eq. (1), when the oxygen motion along the Mn–O bond is considered. The dispersion relation of OW in the A-type antiferromagnetic (AF) phase is calculated by applying the linear spin-wave theory to Eq. (1) and is presented in Fig. 1 (solid curves). A unit cell including four Mn ions is adopted. Spin degree of freedom is assumed to be frozen and effects of spin and spin-orbital coupled excitations are neglected. This is because the characteristic energy of magnon is much lower than that of OW because of competition between ferromagnetic and AF interactions. Dynamical effects of the lattice distortion is

also neglected, since energy of phonon is lower than that of OW in LaMnO₃. Then, the effect of the static Jahn–Teller type lattice distortion in a MnO₆ octahedron is considered by introducing the Jahn–Teller coupling given by $\mathcal{H}_{JT} = -g_{JT} \sum_{i=l=x,z} Q_{il} T_{il}$, where Q_{il} indicates the normal mode of an O₆ octahedron around the Mn ion at site i .

The four OW modes shown in Fig. 1 originate from the four Mn ions included in a unit cell. The parameter values are chosen to be $J_2/J_1 = 0.35$, $g_{JT} \sqrt{Q_x^2 + Q_z^2}/J_1 = 0.7$ and $\tan^{-1}(Q_x/Q_z) = 2\pi/3$. When we focus on the OW at the point Γ in the Brillouin zone, which is detected by the Raman scattering as shown later, the symmetry of the OW is identified by using the group theoretical analyses. The crystal structure of LaMnO₃ shows the space group of D_{2h}^{16} ($Pnma$). The site group for a Mn ion, which is a subgroup of the space group D_{2h} and in which the operations do not move the Mn ion, is C_i . It is shown that electronic excitations between the two e_g orbitals in a Mn site are described by the A_g irreducible representation in C_i . This is reduced into the irreducible representation of the D_{2h} group as $A_g \rightarrow A_g + B_{1g} + B_{2g} + B_{3g}$. Then, the four OW modes at the point Γ have the symmetries of A_g , B_{1g} , B_{2g} , and B_{3g} . The wave function of the A_g and B_{1g} modes are explicitly given by $\psi_{A_g} = 1/2(\psi(0) + \psi(\vec{\tau}_b) + \psi(\vec{\tau}_a + \vec{\tau}_c) + \psi(\vec{\tau}_a + \vec{\tau}_c + \vec{\tau}_b))$ and $\psi_{B_{1g}} = 1/2(\psi(0) + \psi(\vec{\tau}_b) - \psi(\vec{\tau}_a + \vec{\tau}_c) - \psi(\vec{\tau}_a + \vec{\tau}_c + \vec{\tau}_b))$, respectively, where $\psi(\vec{r})$ is the wave function for the orbital excited state at the position \vec{r} and $\vec{\tau}_l = 1/2\hat{a}_l$ ($l = x, y, z$) with the lattice constant \hat{a}_l . As shown in Fig. 1,

OW has a gap which is of the order of J_1 . This gap originates from the A-type AF structure which breaks the cubic symmetry and the coupling with the Jahn–Teller type lattice distortion [5]. We show the dispersion relation of OW in the paramagnetic state in Fig. 1 (dotted curves). The excitation gap is reduced because of the cubic symmetry in the spin structure. This softening of OW also occurs by applying a magnetic field. Both the dispersion relation and the energy gap obtained by the linear spin-wave theory are reproduced by numerical calculations for the dynamical correlation function of the pseudo-spin \tilde{T} , which is obtained by the exact diagonalization method in a small cluster system. This fact implies that, although both $\langle T_{zk} \rangle$ and $\langle T_{xk} \rangle$ are not conserved in the Hamiltonian Eq. (1), the coherent components of the orbital excitations are dominant.

3. Raman scattering from orbital wave

The Raman scattering is one of the experimental techniques to detect the OW in orbital ordered states [6,7]. One of the dominant processes for the Raman scattering from the orbital excitations is caused through the charge transfer excitations between Mn 3d and O 2p orbitals: Consider a pair of the NN Mn and O sites where $e_{g\gamma}$ orbital is occupied by an electron in this Mn site. The incident photon excites an electron in an O 2p orbital to the unoccupied $e_{g-\gamma}$ orbital in the NN Mn site. Then, the electron in the $e_{g\gamma}$ orbital comes back the O 2p orbital with emitting the second photon. This process is described by

$$|e_{g\gamma}(\vec{r})^1\rangle; \rightarrow \left| e_{g\gamma}(\vec{r})^1 e_{g-\gamma}(\vec{r})^1 \underline{p}_x \left(\vec{r} \pm \frac{1}{2} \hat{\delta}_x \right) \right\rangle \rightarrow |e_{g-\gamma}(\vec{r})^1\rangle, \quad (2)$$

where x polarized light is considered. \underline{p}_x indicates the state where one hole occupies the O $2p_x$ orbital, and $\hat{\delta}_x$ is the Mn–O bond length along the x direction. This process excites one OW with zero momentum. This is in contrast to the Raman scattering from the spin wave excitations in antiferromagnet where the one magnon Raman scattering is caused through the spin-orbit coupling in the intermediate scattering states and its intensity is much weaker than that in the two magnon scattering. This difference is attributed to the fact that $\langle \tilde{T}_i \rangle$ is not conserved unlike the spin case. The selection rule of the polarization dependence of the Raman scattering from OW is given by the symmetry of OW. Here, directions being parallel to the a , b and c axes in crystal lattice are denoted by x' , z and y' , respectively, and those being parallel to the $a+c$ and $a-c$ axes are x and y , respectively. The polarization configuration in the Raman scattering is represented as $(\vec{e}_i; \vec{e}_f)$, where $\vec{e}_{i(f)}$ is the polarization vector of the incident (scattered) photon. In this scheme, we derive the selection rules that, for example, the A_g mode is allowed in the configurations of (xx) , (xy) , $(x'x')$ and (zz) , and the B_{1g} modes is in (xx) and $(x'y')$.

The scattering cross-section from OW is given by

$$\begin{aligned} \frac{d^2\sigma}{d\omega_f d\Omega} &= \frac{\omega_f}{\omega_i} \frac{e^4 N}{4} \bar{J}^2 \sum_{\mu} \\ &\times \left| \sum_{\rho\nu} (\vec{e}_f \cdot \vec{\rho})(\vec{e}_i \cdot \vec{\rho}) S_{\nu}^{\rho} (V_{\nu\mu} + W_{\nu\mu}) \right|^2 \\ &\times \{ f_B(\varepsilon_{\mu\vec{k}=0}) \delta(\Delta\omega + \varepsilon_{\mu\vec{k}=0}) \\ &+ (f_B(\varepsilon_{\mu\vec{k}=0}) + 1) \delta(\Delta\omega - \varepsilon_{\mu\vec{k}=0}) \}, \quad (3) \end{aligned}$$

with $\vec{\rho} = \hat{x}$, \hat{y} and \hat{z} . We consider the scattering of photon with energy ω_i and polarization λ_i to that with ω_f and λ_f . The energy transfer is denoted by $\Delta\omega = \omega_i - \omega_f$. $\varepsilon_{\mu\vec{k}}$ is the energy of OW with momentum \vec{k} and mode μ , and f_B is the Bose distribution function. S_{ν}^{ρ} is defined by $S_{\nu}^{\rho} = \sin(\theta_{\nu} + 2\pi m_{\rho}/3)$ with $m_{\rho} = (1,2,3)$ for $\rho = (x,y,z)$ and $\theta_{\nu} = \tan^{-1}(\langle T_{x\nu} \rangle / \langle T_{z\nu} \rangle)$. $V_{\nu\mu}$ and $W_{\nu\mu}$ are coefficients in the Bogolyubov transformation connecting the bosonic operator $a_{\nu\vec{k}}$ at the ν th Mn ion and that $\alpha_{\mu\vec{k}}$ for the μ th OW mode as $a_{\nu\vec{k}=0} = V_{\nu\mu} \alpha_{\mu\vec{k}=0} + W_{\nu\mu} \alpha_{\mu\vec{k}=0}^{\dagger}$. \bar{J} indicates an amplitude of the scattering and the dominant term is given by $3d_{pd}^2 t_{pd}^2 / (\Delta - \omega_f)$ with the bond length d_{pd} and the transfer intensity t_{pd} between NN Mn and O sites and the charge transfer energy Δ .

The calculated Raman spectra from OW is shown in Fig. 2 for several polarization configurations. Here, the small monoclinic lattice distortion is introduced in the orthorhombic crystal structure, which is reported by the detailed chemical analyses [8] and the electron microscopy experiments [9]. Peak structures at around $4.5J_1$ (peak A) and $3.6J_1$ (peak B) originates from OW with the symmetry A_g and B_{1g} , respectively. Intensity of the peak A is larger than the others, because the orbital excitations at the four Mn site in a unit cell are in phase in the A_g mode and the interference effect enhances the scattering intensity. A weak peak at $3.2J_1$ (peak C) is attributed to OW at the point X in the Brillouin zone. This mode becomes Raman active due to the small lattice distortion with the monoclinic symmetry.

The Raman spectra have been recently measured in LaMnO_3 [10]. Three new peak structures are found at about 169, 145 and 125 meV, which are termed peaks α , β and γ , respectively. These are interpreted neither by the two-phonon scattering nor by the magnon scattering because of their symmetry and their energy and temperature dependence. Therefore, the remaining degree of freedom, i.e. the orbital degree of freedom is expected to be the origin of the scattering. The theoretical results of the Raman spectra shown in Fig. 2 show a good agreement with the experimental results; the peak α at 169 meV is observed in the configurations of (xx) , (xy) , $(x'x')$, $(x'y')$ and (zz) , and its intensity is larger than others. On the other hand, peak β at 145 meV is observed in the (xx) , $(x'x')$ and $(x'y')$ configurations and peak γ shows a weak intensity in the (xx) and $(x'x')$ configurations.

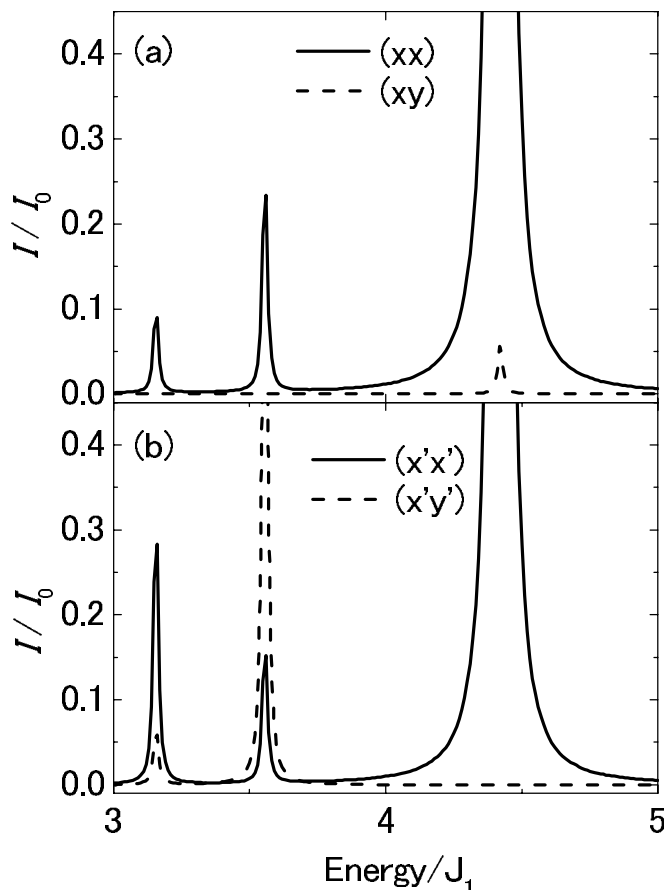


Fig. 2. The Raman scattering spectra from the OW in the A-type AF phase. I_0 is defined by $I_0 = (e^2 N \bar{J} \omega_f) / (4\omega_i)$.

We conclude that the peaks α , β and γ originate from OW corresponding to the peaks A, B and C in the theoretical calculation, respectively.

Acknowledgements

The authors would like to thank Y. Tokura, T. Kimura, E. Saitoh, K. Takahashi, K. Tobe, K. Yamamoto and K. Tsuda for their valuable discussions. This work was supported by Grant-in-Aid for Scientific Research Priority Area from the Ministry of Education, Science, Sports, Culture and Technology of Japan, CREST Japan and Science and Technology Special Coordination Fund for Promoting Science and Technology. One of authors (S.M.) acknowledges support of the Humboldt Foundation.

References

- [1] Y. Tokura, N. Nagaosa, *Science* 288 (2000) 462–467.
- [2] Y. Murakami, H. Kawaka, H. Kawara, M. Tanaka, T. Arima, H. Moritomo, Y. Tokura, *Phys. Rev. Lett.* 80 (1998) 1932–1935.
- [3] S. Ishihara, J. Inoue, S. Maekawa, *Physica C* 263 (1996) 130–133.
- [4] S. Ishihara, J. Inoue, S. Maekawa, *Phys. Rev. B* 55 (1997) 8280–8286.
- [5] S. Ishihara, S. Maekawa, *Phys. Rev. B* 62 (2000) 2338–2345.
- [6] J. Inoue, S. Okamoto, S. Ishihara, W. Koshibae, Y. Kawamura, S. Maekawa, *Physica B* 237–238 (1997) 51–53.
- [7] S. Okamoto, S. Ishihara, S. Maekawa, unpublished, cond-mat/0108032.
- [8] J.F. Mitchell, D.N. Argyriou, C.D. Potter, D.G. Hinks, J.D. Jorgensen, S.D. Bader, *Phys. Rev. B* 54 (1996) 6172–6183.
- [9] K. Tsuda, private communication.
- [10] E. Saitoh, S.O. Kamoto, K.T. Takahashi, K. Tobe, K. Yamamoto, T. Kimura, S. Ishihara, S. Maekawa, Y. Tokura, *Nature* 410 (2001) 180–183.